Table IX. Barriers to Internal Rotation (kcal/mol) in Some Organoborane and the Corresponding Nitro Compounds

	BF_2	ref	NO_2	ref
CH_3XY_2	0.013	12	0.006	29
$CH_3CH_2XY_2$	1.17	11	*a*	
$C_6H_5XY_2$	3.17	25	3.0	28
c-$C_3H_5XY_2$	4.23	this work	4.6	27
$C_2H_3XY_2$	4.17	21	4.83	26

[a] Microwave spectroscopy[30] and matrix and gas-phase infrared spectra[12,31] have shown that the nitro group is undergoing free internal rotation.

Å),[11] and $(CH_3)BF_2$ (1.60 Å).[24] Cyclopropyldifluoroborane, (c-C_3H_5)BF_2 (1.589 Å), would have been expected to fit between phenyldifluoroborane and ethyldifluoroborane if this trend is due to lengthening of the bond as the hybridization of the carbon atom changes from sp to sp^3. However, the uncertainties in the bond length involved would allow for cyclopropyldifluoroborane to take its expected place in the series. The other structural parameters for the BF_2 moiety, r(B–F) = 1.328 ± 0.004 Å and ∠FBF = 115.9 ± 0.9°, are in agreement with those found in CH_3BF_2 (r(B–F) = 1.30 ± 0.02 Å, ∠FBF = 118°),[24] $(C_2H_3)BF_2$ (r(B–F) = 1.331 ± 0.002 Å, ∠FBF = 116.04 ± 0.41°),[4] and $(C_6H_5)BF_2$ (r(B–F) = 1.330 Å, ∠FBF = 116.0°).[25] A possible interaction between the fluorine atom and the eclipsed hydrogen atom results in a tilt of the BF_2 group toward the cyclopropyl ring. We are currently investigating the structure of cyclopropyldimethylborane to ascertain if the observed tilt of the borane moiety is due to a hydrogen–fluorine interaction. Using the method of Penn and Boggs,[14] we obtained a C_2–C_3 bond distance of 1.486 Å. After a diagnostic least-squares analysis was performed the length was determined to be 1.496 Å. This bond length is similar to those found in other compounds containing unsaturated substituents on the ring. The calculations[14] for the bond length in nitrocyclopropane (1.500 Å), *trans*-vinylcyclopropane (1.499 Å), and cyanocyclopropane (1.500 Å) indicate the shortening of this C_2–C_3 bond length.

Also of interest in this study is the barrier to internal rotation of the BF_2 group in cyclopropyldifluoroborane. The barrier has been found to be 4.23 kcal/mol. This is similar to the barrier (4.17 kcal/mol) found in vinyldifluoroborane[21] and slightly higher than the barrier of 3.17 kcal/mol in phenyldifluoroborane.[25] In the corresponding nitro compounds which are isoelectronic with BF_2 compounds, the same trend is visible. A comparison of the barriers of some organoborane compounds and the corresponding nitro compounds is given in Table IX. As shown in the table, nitroethylene (4.83 kcal/mol)[26] and nitrocyclopropane (4.6 kcal/mol)[27] have similar barriers which are higher than the barrier for nitrobenzene (3.0 kcal/mol).[28] It is also interesting to note that the barrier in c-$C_3H_5BF_2$ is so much higher than the barrier in ethyldifluoroborane (1.17 kcal/mol).[11] This large barrier difference clearly indicates a significant mesomeric interaction between the BF_2 moiety and the cyclopropyl ring.

Acknowledgment. The authors gratefully acknowledge the financial support of this study by the National Science Foundation by Grants CHE-77-08310 and CHE-77-10098. We also gratefully acknowledge the assistance of Dr. A. J. Zozulin in obtaining several of the NMR spectra.

---

(26) H. D. Hess, A. Bauder, and Hs. H. Günthard, *J. Mol. Spectrosc.*, **22**, 208 (1967).

(27) S. F. Bush, private communication.

(28) J. H. Høg, L. Nygaard, and G. O. Sørensen, *J. Mol. Struct.*, **7**, 111 (1971).

(29) E. Tannenbaum, R. J. Myers, and W. D. Gwinn, *J. Chem. Phys.*, **25**, 42 (1956).

(30) J. Ekkers, A. Bauder, and Hs. H. Günthard, *Chem. Phys. Lett.*, **22**, 249 (1973).

(31) P. Groner, R. Meyer, A. Gunter, H. Kühne, and Hs. H. Günthard, *Chem. Phys.*, **5**, 136 (1974).

Millimeter Wave Spectrum of Glycine. A New Conformer

R. D. Suenram* and F. J. Lovas

Contribution from the Molecular Spectroscopy Division, National Bureau of Standards, Washington, D.C. 20234. Received June 13, 1980

Abstract: More sensitive observations on the vapor of glycine, the smallest amino acid, have been made in the millimeter region. This work has led to the identification of a second conformer in the gas phase. This conformer has the amino hydrogens hydrogen bonded to the carbonyl oxygen and the hydroxyl hydrogen in the normal cis configuration with respect to the carbonyl group. This new conformer is ≃490 (150) cm^{-1} *lower* in energy than the conformer originally reported. Its spectrum is weaker due to the smaller dipole moment ($\mu_a \simeq 1.00$ (15) D). The distortion fit of 37 transitions yield $A'' = 10341.76$ (17) MHz, $B'' = 3876.195$ (9) MHz, and $C'' = 2912.361$ (10) MHz for the ground state. The excellent agreement between experiment and theory is discussed.

Introduction

In our previous paper on the millimeter wave spectrum of glycine we reported the rotational spectrum of a particular conformer of glycine in the vapor phase (labeled conformer II here).[1] That conformer had a large molecular dipole moment which gave rise to the most intense spectrum of the various possible conformers of glycine in the gas phase. In that report we suggested the possibility that other conformers might be present in larger concentrations than conformer II, but due to smaller electric dipole moments, their rotational spectra might indeed be weaker than the spectrum of II.

Since glycine is the smallest amino acid, it is important to be able to ascertain if more than one conformer exists in the gas phase and, if so, to determine their structural conformations and relative energies. In addition, it is extremely important from an astronomical standpoint to know which conformer is the lowest in energy since in all likelihood the lowest energy conformer will be the most abundant form in cool interstellar dust clouds.

After our previous paper on glycine was published, we made a number of improvements in our spectrometer which have provided improved sensitivity. This paper describes the spectrometer

---

(1) Suenram, R. D.; Lovas, F. J. *J. Mol. Spectrosc.* **1978**, *72*, 372-382.

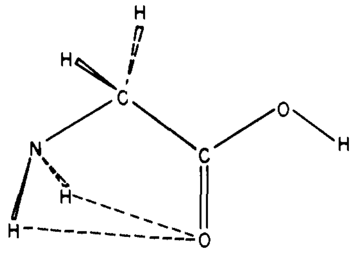

CONFORMER I

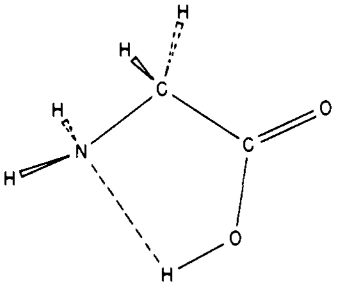

CONFORMER II

currently in use and the observation of the millimeter wave spectrum of the *lowest* energy conformer of vapor-phase glycine.

Experimental Section

A. Automated Spectrometer. In order to have an effective computer-controlled millimeter wave spectrometer, several elements are essential. First, the millimeter wave source (e.g., reflex klystron) must be phase-locked to provide a stable frequency. Second, the source must be frequency tunable in a manner which allows sampling the same discrete points in the spectrum on a repetitive basis. Further, a method of taking, storing, and manipulating data in real time provides flexibility in the system.

The block diagram illustrated in Figure 1 shows the main components of the spectrometer. Phase-locking the millimeter wave klystron is achieved by mixing the klystron frequency with a fixed frequency source (LO). The IF signal is passed through a narrow-banded (100-MHz) 7 stage filter centered at 1090 MHz and amplified to produce a strong beat signal in the 1040–1140-MHz range. This signal is mixed with the output of a computer-controlled synthesizer (980–1080 MHz) in a double-balanced mixer. The difference frequency (60 MHz) obtained from the double-balanced mixer is input to a phase-locking synchronizer modified as described by Pickett.[2] The synchronizer in turn applies correction voltage to the klystron repeller to keep it phase-locked at the desired frequency. The bandwidth of this system allows one to scan 50–80 MHz without difficulties in maintaining a stable phase-lock with stepping speeds of a few milliseconds and step sizes up to 1 MHz.

B. Design of a Medium-Temperature Millimeter Cell. The cell used in the previous study had a number of disadvantages which we felt could be overcome by the design and construction of a new cell. The new cell shown in Figure 2 is approximately 1 m long and is of the parallel plate design. The cell was constructed to allow all internal surfaces to be heated. When glycine is vaporized in the center section, it migrates to the ends of the cell and down into the traps which are at room temperature and only at this point can it condense out. This allows a slow continuous flow to be established. With this arrangement it was possible to work several weeks with a single charge of 10–15 g of glycine. As in the previous cell, all metal surfaces were gold plated to minimize decomposition.

Heating was accomplished with several heating tapes wrapped around the glass vacuum envelop and a separate heating tape around the sample region. For most experiments, all regions of the cell were maintained at ≃200 °C except the sample region which was maintained between 170 and 180 °C.

Spectral Predictions

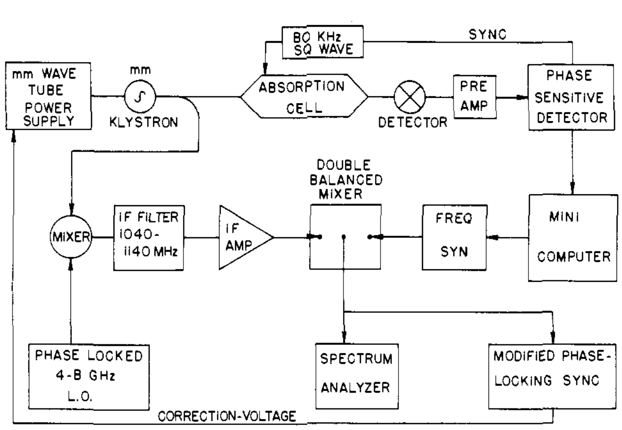

Figure 1. Block diagram of the millimeter wave spectrometer employed in the present study.

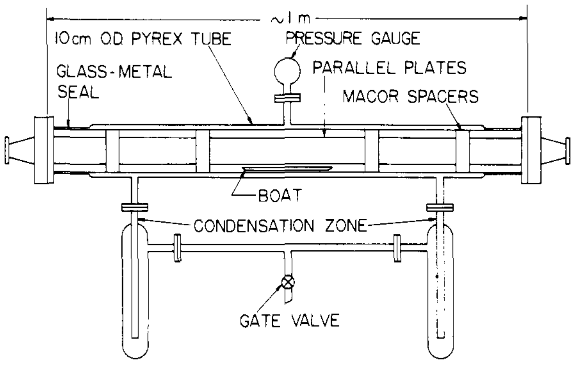

Figure 2. Schematic drawing of the heated absorption cell used in this study.

One of the greatest aids to the assignment of the rotational spectrum of a molecule is the ability to accurately predict the frequencies of the spectral lines. Usually this is done from an estimated geometric structure, and the predictions are only as good as the "estimated structure". Since glycine is the smallest amino acid, considerable effort has been devoted to its structural determination by theoretical chemists.[3-6] These efforts have focused not only on conformational analysis and relative energy determinations[3,4] but also on the complete geometry optimization of several of the lowest energy conformers.[5,6] The excellent agreement between the observed and calculated rotational constants for structure II[1,5] led us to favor spectral predictions on the basis of geometry-optimized structure of Sellers and Schäfer for structure I also.[5]

From this structure, one predicts A = 10300.8 MHz, B = 3890.3 MHz, and C = 2917.8 MHz. Furthermore, the largest molecular dipole moment component is expected to lie along the a principal axis. Thus one would expect to see the spectrum of a slightly asymmetric prolate rotor. In this type of spectrum, the strong a-type R-branch transitions occur in clusters spaced by $\simeq(B + C)$ which for glycine is about 7 GHz. This type of spectral pattern was observed earlier for II, but for I, the value of $B + C$ is predicted to be slightly different so that these same transitions fall in the relatively sparse region between the clusters of II. This is a rather fortunate situation since the spectrum of I was expected to be substantially weaker than the spectrum of II due to the large difference in calculated molecular dipole moments (approximately 6.5:1.0). Since the intensities of rotational transitions are proportional to the square of the dipole moment, II was predicted to enjoy about a 40:1 advantage over I in line intensities. Thus, even if I were more abundant than II in the gas phase, the spectrum could be weaker.

On the basis of the preceding arguments, regions from 81.40–83.40 GHz and 88.65–90.40 GHz were scanned by using the computer-controlled spectrometer. These were the regions where the fast modulating intermediate and high K_{-1} doublets of

---

(2) Pickett, H. M. *Rev. Sci. Instrum.* **1977**, *48*, 706–707.

(3) Oegerle, W. R.; Sabin, J. R. *J. Mol. Struct.* **1973**, *15*, 131–136.

(4) Vishveshwara, S.; Pople, J. A. *J. Am. Chem. Soc.* **1977**, *99*, 2422–2426.

(5) Sellers, H. L.; Schäfer, L. *J. Am. Chem. Soc.* **1978**, *100*, 7728–7729.

(6) Schäfer, L.; Sellers, H. L.; Lovas, F. J.; Suenram, R. D. *J. Am. Chem. Soc.* **1980**, *102*, 6566.

Table I. Rotational Transitions of Glycine Conformer I in the Ground Vibrational State[a]

$J'_{K_-',K_+'}-J''_{K_-'',K_+''}$	measd freq, MHz	obsd – calcd, MHz
$12_{10}-11_{10}$[b]	81 940.77	0.16
$12_{9}-11_{9}$	82 011.88	−0.06
$12_{8}-11_{8}$	82 111.68	0.09
$12_{7,6}-11_{7,5}$	82 258.00[c]	0.12
$12_{7,5}-11_{7,4}$		−0.17
$12_{6,7}-11_{6,6}$	82 484.46[d]	0.37
$12_{6,6}-11_{6,5}$	82 492.78[d]	−0.57
$12_{5,8}-11_{5,7}$	82 806.14	0.07
$12_{4,9}-11_{4,8}$	82 866.89	−0.04
$12_{5,7}-11_{5,6}$	82 982.40	−0.06
$13_{1,12}-12_{1,11}$	84 130.90	0.04
$14_{0,14}-13_{1,13}$	84 204.25[e]	0.10
$14_{1,14}-13_{1,13}$	84 217.94	0.01
$14_{0,14}-13_{0,13}$	84 230.25	0.00
$14_{1,14}-13_{0,13}$	84 244.01[e]	−0.02
$12_{2,10}-11_{2,9}$	84 813.25	0.00
$13_{11}-12_{11}$	88 755.84	0.09
$13_{10}-12_{10}$	88 822.86	−0.16
$13_{9}-12_{9}$	88 913.45	−0.07
$13_{8}-12_{8}$	89 040.30	0.02
$13_{7,7}-12_{7,6}$	89 227.45[c]	0.67
$13_{7,6}-12_{7,5}$		−0.24
$13_{6,8}-12_{6,7}$	89 513.50[d]	1.27
$13_{6,7}-12_{6,6}$	89 535.97[d]	0.44
$13_{5,9}-12_{5,8}$	89 875.80	0.05
$15_{0,15}-14_{1,14}$	90 036.02[e]	0.07
$15_{1,15}-14_{1,14}$	90 043.13	−0.04
$15_{0,15}-14_{0,14}$	90 049.71	−0.02
$15_{1,15}-14_{0,14}$	90 056.98[e]	0.03
$13_{5,8}-12_{5,7}$	90 233.63	−0.07
$13_{3,10}-12_{3,9}$	94 211.95	−0.06
$16_{15}-15_{15}$	109 149.20	0.00
$16_{14}-15_{14}$	109 198.42	0.02
$16_{13}-15_{13}$	109 258.42	0.05
$16_{12}-15_{12}$	109 332.97	−0.05
$16_{11}-15_{11}$	109 428.04	−0.13
$16_{10}-15_{10}$	109 552.85	−0.01
$16_{9}-15_{9}$	109 721.84	0.03
$16_{4,13}-15_{4,12}$	109 824.30	0.10
$16_{8,9}-15_{8,8}$	109 960.53[c]	0.20
$16_{8,8}-15_{8,7}$		−0.49
$16_{7,10}-15_{7,9}$	110 311.16	0.25
$16_{7,9}-15_{7,8}$	110 326.32	−0.19
$16_{6,11}-15_{6,10}$	110 791.85	0.00
$16_{6,10}-15_{6,9}$	111 023.90	0.12
$16_{5,12}-15_{5,11}$	111 042.04	−0.01
$17_{3,15}-16_{3,14}$	112 250.70	−0.21
$18_{2,17}-17_{2,16}$	112 887.45	0.17
$18_{1,17}-17_{1,16}$	112 925.70	−0.07
$16_{5,11}-15_{5,10}$	112 962.05	−0.05
$17_{2,15}-16_{2,14}$	113 156.00	0.03

[a] Typical measured uncertainties were 0.1–0.2 MHz. [b] When K_{oblate} is omitted, the transition exists as a degenerate doublet and only one of the degenerate pair is included in the fit. [c] This pair of transitions were observed to be unsplit and were not included in the fit. The predicted splitting was small but not zero so they were not fit. [d] Not included in the fit due to an overlap of transitions or small perturbation. [e] These four *b*-type transitions have been observed but are not included in the fit.

Table II. Rotational Transitions of Glycine Conformer I in Several Excited Torsional States[a]

$J'_{K_-',K_+'}-$ $J''_{K_-',K_+''}$	measd freq $\upsilon = 1$, MHz	obsd – calcd, MHz	measd freq $\upsilon = 2$, MHz	measd freq $\upsilon = 3$, MHz
$12_{9}-11_{9}$[b]	82 069.20	0.10		
$12_{8}-11_{8}$	82 168.50[c]	0.58		
$12_{7,6}-11_{7,5}$	82 312.94[d]	−0.05		
$12_{7,5}-11_{7,4}$		−0.34		
$12_{6,7}-11_{6,6}$	82 537.28	−0.04		
$12_{6,6}-11_{6,5}$	82 546.18	−0.30		
$12_{5,8}-11_{5,7}$	82 857.25[c]	0.52	82 900.30	
$12_{5,7}-11_{5,6}$			83 072.94	
$12_{4,9}-11_{4,8}$	82 917.71	0.00		
$12_{5,7}-11_{5,6}$	83 031.50	0.21		
$12_{4,8}-11_{4,7}$	84 587.91	0.06		
$13_{11}-12_{11}$	88 817.75[c]	−0.67		
$13_{10}-12_{10}$	88 885.15	0.06		
$13_{9}-12_{9}$	88 975.00[c]	0.16	89 010.00	
$13_{8}-12_{8}$	89 100.50	−0.05		89 173.50
$13_{7,7}-12_{7,6}$	89 285.63[d]	0.12		89 364.50
$13_{7,6}-12_{7,5}$		−0.77		
$13_{6,8}-12_{6,7}$	89 568.90	0.31	89 609.50	
$13_{4,10}-12_{4,9}$	89 805.85	−0.24		
$13_{5,9}-12_{5,8}$	89 929.20	−0.11	89 975.15	90 020.32
$13_{5,8}-12_{5,7}$	90 283.50	−0.09	90 325.25	90 374.30
$14_{3,12}-13_{3,11}$	94 125.90	0.11		
$13_{3,10}-12_{3,9}$	94 232.78	0.02		
$16_{13}-15_{13}$	109 335.20	0.12		
$16_{12}-15_{12}$			109 476.80	
$16_{11}-15_{11}$	109 503.54	0.04	109 570.25	
$16_{10}-15_{10}$	109 626.94	−0.22	109 693.04	110 747.00
$16_{9}-15_{9}$	109 794.52	−0.22	109 858.89	109 915.00
$16_{4,13}-15_{4,12}$	109 898.84	0.07		
$16_{8,9}-15_{8,8}$	110 031.74[d]	0.45	110 093.81	110 155.60
$16_{8,7}-15_{8,6}$		−0.23		
$16_{7,10}-15_{7,9}$	110 379.06	0.07	110 437.50	110 509.86
$16_{7,9}-15_{7,8}$	110 394.36	−0.03	110 452.50	110 526.04
$16_{6,10}-15_{6,9}$	111 085.70	0.16		
$16_{5,12}-15_{5,11}$	111 105.22	−0.01		

[a] Only the transitions from the $\upsilon = 1$ state were fit to the CD model. Those from $\upsilon = 2$ and $\upsilon = 3$ were not fit and are included here for future reference. Transitions from $\upsilon = 1$ as well as $\upsilon = 2$ and $\upsilon = 3$ were used to determine the torsional energy level separation. Measured uncertainties are 0.1 MHz for $\upsilon = 1$ and 0.2 MHz for $\upsilon = 2$ and 3. [b] When K_{oblate} is omitted, the transitions exist as a degenerate pair and only one of the pair was fit. [c] These transitions were either overlapped or show slight perturbations and were thus not included in the fit. [d] In the experiment, these transitions were observed as one line. The predicted splitting is small but nonzero, so they were not included in the fit.

the $J = 12 \leftarrow 11$ and $J = 13 \leftarrow 12$ *a*-type clusters were predicted to occur. A number of weak transitions were observed in these regions which appeared to have much narrower line widths than the transitions from II, which were quite broad. Everything looked consistent with the spectral precitions, but an assignment eluded us at this point due primarily to the weakness of the observed features and the overlap of several transitions from the ground and excited vibrational states of II. In order to obtain more data, we made spectral scans from 109.20 to 110.60 GHz. In this region, the degenerate $J = 16_9-15_9$ and $J = 16_8-15_8$ transitions of the ground state and several vibrational states were observed. In addition, the slightly split $16_{7,10}-15_{7,9}$ and $16_{7,9}-15_{7,8}$ transitions were identified. This provided the basis for an assignment which then allowed further assignment of transitions in the two lower frequency regions. Eventually, 37 *a*-type transitions were measured for the ground state and fitted to the centrifugal distortion model of Watson by using the computer program developed by Kirchhoff.[7,8] The transitions that were fitted are shown in Table I.

In addition to the ground-state spectrum, a prominent series of excited vibrational state transitions was also readily apparent. Transitions from the first excited state were also fitted to the centrifugal distortion model. Transitions from excited states through $\upsilon = 3$ were also observed but could not be fitted to a centrifugal distortion model due to a lack of sufficient data. The transitions for $\upsilon = 1$, 2, and 3 are shown in Table II. The sepctroscopic constants for the ground state and $\upsilon = 1$ are shown in Table III.

Dipole Moment Determination

Due to the weakness of the transitions and the fact that the observed transitions have high J values, determination of the electric dipole moment in the usual fashion was not feasible since individual M_J Stark components were too weak to assign with

---

(7) Watson, J. K. G. *J. Chem. Phys.* **1967**, *46*, 1935–1949.
(8) Kirchhoff, W. H. *J. Mol. Spectrosc.* **1972**, *41*, 333–380.

Table III. Rotational Constants, Nonplanar Moments, and Centrifugal Distortion Parameters for Glycine Conformer I in the Ground and First Excited Torsional States

	ground state	$v = 1$ state
A'', MHz	10341.76 (17)[a]	10294.06 (63)
B'', MHz	3876.195 (9)	3874.984 (51)
C'', MHz	2912.361 (10)	2918.745 (69)
τ_1, kHz	−24.84 (13)	−24.45 (78)
τ_2, kHz	−6.003 (99)	−5.78 (43)
τ_3, kHz[b]	75 (10)	109 (42)
τ_{aaaa}, kHz	−36 (30)	c
τ_{bbbb}, kHz	−4.604 (90)	−4.25 (54)
τ_{cccc}, kHz	−1.61 (11)	−2.8 (10)
$I_a + I_b - I_c$, u Å^2	5.719	6.366

[a] The numbers in parentheses are the standard deviations of the fit and refer to the last digit(s) given. [b] τ_3 is fixed by setting $R_6 = 0$ (see ref 8). [c] τ_{aaaa} was not fit for $v = 1$ since for the measured transitions there is a high degree of correlation with the A rotational constant.

certainty. An alternative approach was employed, the rate of growth technique in which the percent modulation of a given transition was measured as a function of the applied electric field. The $13_{5,8}$–$12_{5,7}$ transition was chosen since it is readily modulated at low fields, and the μ_a term in the second-order behavior is dominant for all the M_J levels except $M_J = 0$. With use of this method, 18 scans were taken at different electric field values. The percent modulation at each field setting was determined by dividing the observed intensity by the line intensity of the fully modulated line. The Stark cell was calibrated by using the first-order Stark component ($\Delta M_J = 0$) of the $1_1 \rightarrow 2_1$ transition of methyl fluoride at 102140.87 MHz.[9] The electric dipole moment of CH_3F was taken from Wolfsy et al.[10] where they determined: $\mu = 1.8585(5)$ D. Since no dc bias voltage was applied, the 80 kHz square wave was rectified into a dc voltage and read directly on a digital voltmeter. Both the calibration and the glycine measurements were performed in this fashion to minimize systematic errors.

A family of theoretical curves was generated by calculating the percent modulation vs. field for a number of values of μ_a. These were plotted on a log–log scale (Figure 3) for $\mu_a = 0.8$, 1.0, and 1.2 D along with the experimental curve. Although crude, this method provided the best determination of μ_a possible under our experimental conditions. From the graph one concludes $\mu_a \simeq 1.0 \pm 0.15$ D. It is interesting to note that this number is qualitatively in agreement with the theoretical value obtained by Sellers and Schäfer[5] which is listed in Table V. Sellers and Schäfer also calculate a small value for μ_b. As can be seen from Table I, we have observed four transitions which are in excellent agreement with the predicted frequencies of four *b*-type lines. If these assignments are correct, this indicates that $\mu_b \neq 0$, but in any case, $\mu_a > \mu_b$.

Vibrational Energy Determination

The vibrational energy level separation was determined by carefully measuring the relative intensities of the $K_{-1} = 8$ and 9 levels of the $J = 16$–15 transitions in the 109-GHz region. Intensities of vibrational state transitions up to $v = 3$ were used. In this determination only the peak intensity was used to obtain the relative intensity since the line widths for the ground state and vibrational states were approximately equal. The temperature of the molecules was taken to be the same as that of the parallel plates in the cell which were at 200 °C. Various combinations between the ground state and vibrational states were determined for these two transitions and an average taken to yield $\Delta E = 62 \pm 20$ cm^{-1}. Since the nonplanar moment increases on going from the ground state to the excited vibrational state, the vibration in question must be an out of plane torsion, probably about the C–C bond. This is consistent with C–C torsional frequency found by Stiefvater in the analogous conformer of propionic acid (64 ± 3 cm^{-1})[11].

Table IV. Parameters for the $13_{5,8}$–$12_{5,7}$ Transitions of Both Conformers of Glycine[a]

conformer	ν, MHz	fwhm, MHz	peak intensity, arb units	electric field, V/cm	no. of scans
I	90233.63 (10)	1.48	127	1400	18
II	94719.70 (20)	4.10	238	800	10
		$\gamma_{II}'/\gamma_I' = 5.2$			

[a] The temperature of the molecules was assumed to be equal to the temperature of the plates which was 200 °C.

Energy Difference between Conformers

One of the most important objectives of this study was the determination of the energy difference between the two glycine conformers. To accomplish this, intensity measurements were made on the $13_{5,8}$–$12_{5,7}$ transition of both conformers. The total intensity of a rotational transition can be expressed as eq 1. In

$$\gamma = \kappa f_v N \sqrt{ABC}(e^{-W_R/kT})(2J + 1)\mu_a^2(\nu^2/\Delta\nu) \qquad (1)$$

the equation γ is the measured intensity and κ is a constant which contains a number of the universal constants. The vibrational partition function, f_v, was not evaluated but was assumed to be equal for both conformers. This is a valid assumption since the major contribution of f_v comes from vibrational modes with frequencies less than about 500 cm^{-1} and both conformers have similar low-frequency torsional motions in this frequency range. N is the total number of molecules/cm^3. A, B, and C are the rotational constants, $e^{-W_R/kT}$ is the Boltzman factor for the rotational partition function, μ_a is the molecular electric dipole moment along the a principal axis, ν is the frequency of the transition in question, and $\Delta\nu$ is the line width. With the above assumptions included and taking the ratio, eq 1 simplies to eq 2.

$$\frac{\gamma_{II}}{\gamma_I} = \frac{(\sqrt{ABC}(e^{-W_R/kT})\mu_a^2(\nu^2/\Delta\nu))_{II}}{(\sqrt{ABC}(e^{-W_R/kT})\mu_a^2(\nu^2/\Delta\nu))_I} \frac{N_{II}}{N_I} \qquad (2)$$

Generally $\Delta\nu$ is taken to be the same for both conformers. Here, however, it is not possible since the line widths differ greatly due to the large difference in dipole moments. Therefore, the integrated intensity was used to determine the total line intensity. Thus γ is redefined as $\gamma_i' = \gamma_i \Delta\nu_i$. If thermal equilibrium is assumed, the ratio of N_{II}/N_I is equal to the Boltzman factor, $e^{-W_c/kT}$, where W_c is the energy difference between the 0_{00} levels of conformers I and II. Including these terms and rearranging we get eq 3, which is used to determine the energy level separation.

$$W_c = -kT \ln \left[\left(\frac{\gamma_{II}'}{\gamma_I'} \right) \frac{(\sqrt{ABC}(e^{-W_R/kT})\mu_a^2\nu^2)_I}{(\sqrt{ABC}(e^{-W_R/kT})\mu_a^2\nu^2)_{II}} \right] \qquad (3)$$

Table IV summarizes the data for the transitions used in the relative energy determination. In both cases Gaussian curves were fitted to the absorption lines to get the full width at half-height ($\Delta\nu$) and relative peak intensity. The value for the energy separation is ≃490cm^{-1} with I being *lower* in energy than II.

There are two independent sources of error in the relative energy measurements. The first is the uncertainity associated with overall relative sensitivity of the spectrometer at the two different frequencies. The magnitude of this uncertainty is probably less than 10%. The larger uncertainty is due to the error associated with the dipole moment measurement of I, which gives rise to ≃100-cm^{-1} uncertainty. Adding these together gives 490 ± 150

---

(9) Larkin, D. M.; Gordy, W. *J. Chem. Phys.* **1963**, *38*, 2329–2333.

(10) Wofsy, S. C.; Muenter, J. S.; Klemperer, W. *J. Chem. Phys.* **1971**, *55*, 2014–2019.

(11) Stiefvater, O. L. *J. Chem. Phys.* **1975**, *62*, 233–243.

(12) Townes, C. H.; Schawlow, A. L. "Microwave Spectroscopy", McGraw-Hill: New York, 1955; pp 101–102.

Table V. Comparison of Experimental Results with Ab Initio Calculations for the Low-Energy Conformers of Glycine

	conformer I		conformer II		conformer III
	expt[a]	theory[b]	expt[c]	theory[b]	theory[b]
A^d	10341.76 (17)	10300.8	10130.47 (62)	10095.4	9949.6
B	3876.195 (9)	3890.3	4071.473 (36)	4107.6	4052.0
C	2912.361 (10)	2917.8	3007.538 (44)	3021.0	2976.6
$\mu_a{}^e$	1.0 ± 0.15	1.0	4.5[f]	6.4	0.3
$\mu_b{}^e$	>0	0.5		1.4	1.7
E, cm^{-1}	0	0	490 ± 150[a] cm^{-1}	770 [350][g] cm^{-1}	665 cm^{-1}

[a] This work. [b] The rotational constants, dipole moments, and energies under the "theory" heading were calculated by using the data presented in ref 5 and 6. [c] These rotational constants are from ref 1. [d] The units on all rotational constants are megahertz. [e] All dipole moment values are in Debye. [f] Reference 14. [g] The value in brackets is an estimate of the energy difference after taking into account approximate energy differences due to zero point effects. For details see ref 5.

cm^{-1} as the energy level separation.

Discussion

At this point it is probably worth considering all of the experimental evidence to convince ourselves that the observed conformer is indeed the one represented as I. As mentioned in the first paper on glycine, it is difficult to make assumptions about different conformers of glycine solely on the basis of comparisons with estimated structures since all conformers have similar rotational constants. One must rely also on the nonplanar moment $\Delta = I_a + I_b - I_c$ and the molecular dipole moment. The nonplanar moment for the ground state of the observed conformer is $\Delta = +5.719$ u Å^2 which is consistent with a planar heavy-atom structure, with the two methylene and two amino hydrogens symmetrically placed out of the a, b plane. This narrows the number of possibilities to the eight configurations which have all heavy atoms in the symmetry plane.[13] Of these eight, one has already been determined to be II so there are seven remaining choices. Several of these can be readily eliminated by considering the relative energy as calculated by Vishveshwara and Pople.[4]

After this is done, the two reasonable choices that remain are I and III. I is certainly the favored choice because it is calculated to be the lowest energy conformer and the newly assigned species is ≃490 cm^{-1} lower in energy than II which is qualitatively the amount also predicted by Vishveshwara and Pople.[4] Once the choice has been narrowed to two, it becomes feasible to increase the level of sophistication of the ab initio calculations and to optimize the geometry to obtain the "best" structure for each of I, II, and III. These calculations have recently been reported by Schäfer et al.[6] The results of these calculations are summarized in Table V. A comparison of the experimental and theoretical constants in Table V indicates that the obvious choice for the newly assigned conformer is indeed I. The agreement between the experimental rotational constants and those calculated from theory for I and II is extremely good and lends confidence to the assignment of the glycine spectrum reported here to conformer I and the spectrum reported earlier[1] to II as originally suggested.

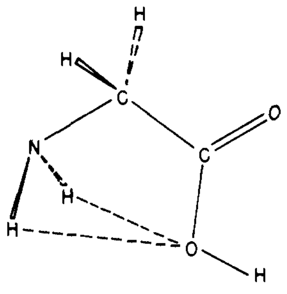

CONFORMER III

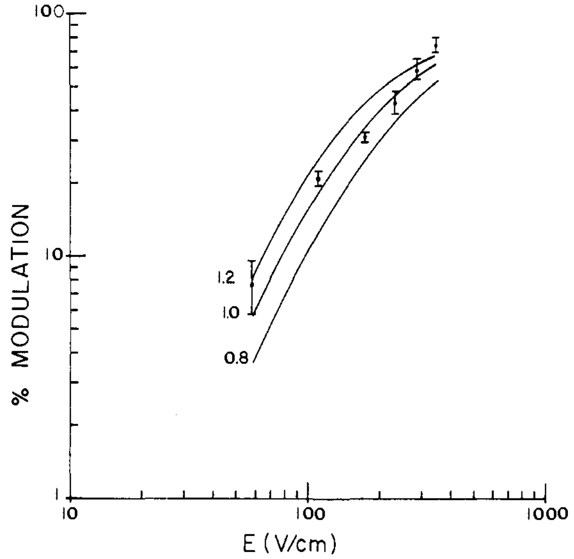

Figure 3. log–log plot showing the data used for the determination of the dipole moment of I.

It is gratifying that the theoretical work and the experimental data are now in agreement and that the apparent anomaly concerning the lowest energy form of glycine in the gas phase has been resolved.[1,5,6,14] As mentioned earlier, this is an extremely important matter from an astronomical point of view. This paper provides the basis to begin the astronomical search for conformer I, the most likely conformer of glycine to exist in cool interstellar dust clouds.

Acknowledgment. The authors would like to thank Dr. J. M. Hollis for his able assistance in the software development for the data acquisition system. We would also like to thank Dr. Hollis and Professor L. E. Snyder for continued encouragement throughout the course of this work. Dr. H. M. Pickett is gratefully acknowledged for his assistance and guidance in the design and modifications of some of the electronic components which improved the phase-lock system.

The many technical discussions with Dr. G. G. Luther, Professor R. L. Kuczkowski, and Dr. R. F. Wormsbecher were also highly beneficial.

---

(13) For further clarification of this point see Table V in ref 1.

(14) Brown, R. D.; Godfrey, P. D.; Storey, J. W. V.; Bassez, M. P. *J. Chem. Soc., Chem. Commun.* **1978**, 547–548.